International Journal of Nanomedicine

Dovepress
open access to scientific and medical research

Open Access Full Text Article

ORIGINAL RESEARCH

Chitosan/siRNA functionalized titanium surface via a layer-by-layer approach for in vitro sustained gene silencing and osteogenic promotion

This article was published in the following Dove Press journal:
International Journal of Nanomedicine
24 March 2015
Number of times this article has been viewed

Wen Song[1,*]
Xin Song[2,*]
Chuanxu Yang[2]
Shan Gao[2]
Lasse Hyldgaard Klausen[2]
Yumei Zhang[1]
Mingdong Dong[2]
Jørgen Kjems[2]

[1]State Key Laboratory of Military Stomatology, Department of Prosthetic Dentistry, School of Stomatology, The Fourth Military Medical University, Xi'an, People's Republic of China; [2]Interdisciplinary Nanoscience Center (iNANO), Aarhus University, Aarhus, Denmark

*These authors contributed equally to this work

Abstract: Titanium surface modification is crucial to improving its bioactivity, mainly its bone binding ability in bone implant materials. In order to functionalize titanium with small interfering RNA (siRNA) for sustained gene silencing in nearby cells, the layer-by-layer (LbL) approach was applied using sodium hyaluronate and chitosan/siRNA (CS/siRNA) nanoparticles as polyanion and polycation, respectively, to build up the multilayered film on smooth titanium surfaces. The CS/siRNA nanoparticle characterization was analyzed first. Dynamic contact angle, atomic force microscopy, and scanning electron microscopy were used to monitor the layer accumulation. siRNA loaded in the film was quantitated and the release profile of film in phosphate-buffered saline was studied. In vitro knockdown effect and cytotoxicity evaluation of the film were investigated using H1299 human lung carcinoma cells expressing green fluorescent protein (GFP). The transfection of human osteoblast-like cell MG63 and H1299 were performed and the osteogenic differentiation of MG63 on LbL film was analyzed. The CS/siRNA nanoparticles exhibited nice size distribution. During formation of the film, the surface wettability, topography, and roughness were alternately changed, indicating successful adsorption of the individual layers. The scanning electron microscope images clearly demonstrated the hybrid structure between CS/siRNA nanoparticles and sodium hyaluronate polymer. The cumulated load of siRNA increased linearly with the bilayer number and, more importantly, a gradual release of the film allowed the siRNA to be maintained on the titanium surface over approximately 1 week. In vitro transfection revealed that the LbL film-associated siRNA could consistently suppress GFP expression in H1299 without showing significant cytotoxicity. The LbL film loading with osteogenic siRNA could dramatically increase the osteogenic differentiation in MG63. In conclusion, LbL technology can potentially modify titanium surfaces with specific gene-regulatory siRNAs to enhance biofunction.

Keywords: sustained gene silencing, osteogenic differentiation, chitosan, small interfering RNA, titanium

Introduction

Titanium and its alloys are widely used in clinical implant materials due to the excellent compatibility and osseointegrative ability. Numerous efforts have been applied to modify the titanium surface to acquire enhanced bioactivity. To simulate bone-like apatite surfaces, hydroxyapatite films are often studied.[1,2] Sandblasting and acid etching can roughen the surface of titanium implants and strengthen the implant fixation as well.[3] Micro-arc oxidation represents another documented technique for improving titanium biocompatibility.[4] In our previous research, we systematically studied how the topography of the titanium surface affects osteoblastic cells. Briefly, the hybrid micropitted/nanotubular topographies, fabricated by acid etching and anodize oxidation on titanium surfaces, could simulate native bone hierarchical extracellular matrix

Correspondence: Yumei Zhang
State Key Laboratory of Military Stomatology, Department of Prosthetic Dentistry, School of Stomatology, The Fourth Military Medical University, No 145 West Changle Road, Xi'an 710032, People's Republic of China
Email wqtzym@fmmu.edu.cn

Jørgen Kjems
Aarhus University, Gustav Wieds Vej 14, 8000 Aarhus C, Denmark
Email jk@mb.au.dk

(ECM) and result in better biological performance in both mesenchymal stem cell and osteoblast model systems.[5,6] However, it is essential to consider that titanium is an inorganic material, and multiple interactions can happen between biomacromolecules and the titanium implant.[7] Consequently, immobilization of biomolecules onto titanium is a novel solution to functionalize the surface. Among various functional biomolecules, the ECM components of the adjacent tissue are mostly likely to immobilize to titanium implants after implant insertion.[8] In addition, therapeutic agents such as bisphosphonates[9] and vancomycin[10] have also been introduced onto titanium surfaces to promote osseointegration or antibacterial effect. From the molecular biology viewpoint,[11] this is an attractive possibility if the gene expression program in adjacent cells could be regulated locally.

RNA interference (RNAi) is a crucial posttranscriptional gene silencing process mediated either by synthetic small interfering RNAs (siRNAs) or endogenous microRNAs. RNAi is well established as an efficient tool for investigation of gene function and therapeutic application in various diseases due to its high specificity of target gene silencing.[12,13] It might, therefore, be possible to introduce the siRNA onto titanium surfaces to biofunctionalize the implants. Previously, Joddar et al immobilized siRNA onto a dopamine-coated stainless steel surface to make specifically sustained Egr-1 knockdown.[14] However, application of siRNA to titanium implants has not been studied. Here, we applied the layer-by-layer (LbL) self-assembly technique to immobilize siRNA onto titanium surfaces. This is a well-established favorable approach to fabricating multilayered film on material surface via electrostatic adsorption, practically accomplished by sequentially dipping the substrate into polyanion and polycation solutions. The method has successfully been used to deliver growth factors,[15] DNA molecules,[16,17] RNA molecules,[18] and other therapeutic drugs[19] from substrate surface. More importantly, LbL delivery of siRNA has been the target of considerable studies.[20,21] The advantage of multilayered film is the potential of controlled loading and release profiles, which is pivotal to clinical requirement of prolonged effects.

In the present study, we chose chitosan (CS)/siRNA nanoparticles as positive charged polymer since naked siRNA is small, which is not convenient for building LbL directly. Meanwhile, the commonly used hyaluronic acid (HA) acted as negative charged polymer.[22] Contact angle measurement, surface topography, and fluorescence observation were applied to monitor the growth of the coating and the amount of siRNA in the film growth process, and the release assay was quantified. The human non-small-cell lung carcinoma cell line, H1299, with endogenous green fluorescent protein (GFP) expression was used to evaluate the gene silencing effect of LbL-incorporated siRNA targeting the expression of GFP (siGFP) because the cells had a strong capacity for endocytosis. An osteogenic siRNA that targets casein kinase-2 interacting protein-1 (siCkip-1)[23] was encapsulated into the LbL film to observe the osteogenic differentiation in human osteoblast-like cell MG63.

Materials and methods

Materials

Titanium-coated silicon wafer (0.5×0.5 cm) was produced by vapor deposition as a gift from the Interdisciplinary Nanoscience Center (iNANO). CS (150 kDa, 95% deacetylation) was provided by HEPPE MEDICAL (Halle, Germany). Sodium hyaluronate (Mw ≈360 kDa) was purchased from Life-core Biomedical, LLC (Chaska, MN, USA). Polyethylenimine ([PEI] Mw 750 kDa, 50 wt% solution), β-glycerophosphate, ascorbic acid, and dexamethasone were obtained from Sigma-Aldrich Co. (St Louis, MO, USA). siRNA duplex targeting murine TNF-α (siTNF) sequence (sense, 5'-pGUCUCAGCCUCUUCUCAUUCCUGct-3', antisense, 5'-AGCAGGAAUGAGAAGAGGCUGAGACAU-3') and siGFP sequence (sense, 5'-GACGUAAACGGCCACAAGUUC-3', antisense: 5'-ACUUGUGGCCGUUUACGUCGC-3') were bought from Dharmacon (Lafayette, CO, USA). siRNA duplex targeting human Ckip-1 sequence (sense, 5′- CGCACAGUCAGUACCGGAAdT*dT-3′, antisense, 5′- UUCCGGUACUGACUGUGCGdT*dT-3′) was ordered from GenePharma (Shanghai, People's Republic of China). Hoechst dye, RiboGreen® kit, Lipofectamine® 2000, and alamarBlue® were bought from Thermo Fisher Scientific (Waltham, MA, USA). BCIP/NBT Alkaline Phosphatase Color Development Kit, Sirius Red, and Alizarin Red were bought from Leagene (Beijing, People's Republic of China).

CS/siRNA nanoparticle formulation and characterization

CS was dissolved in sodium acetate buffer (0.2 M, pH 5.5) overnight at a concentration of 0.8 mg/mL and sterilized using a 0.2 μm syringe filter. To obtain the CS/siRNA nanoparticles, 20 μL siRNA (100 μM in RNase-free water) was added dropwise into 1 mL CS solution with magnetic stirring for 30 minutes at room temperature.[24] The N/P ratio (the molar ratio of CS amino groups to siRNA phosphate groups) was calculated with a mass per phosphate of 325 Da of siRNA, and mass per charge of CS was 163 (95% deacetylation). In our experiment, the N/P ratio was 60. In the characterization test, siTNF was used to form the

nanoparticles. The size was measured based on dynamic light scattering using a Zetasizer Nano ZS (Malvern Instruments, Malvern, UK). Briefly, 100 μL particle solution was added into a cuvette and the size was measured at a temperature of 20°C three times to acquire a statistical result. The morphology of particles was observed using a transmission Tecnai electron microscope, FEI (Hillsboro, OR, USA). In concision, 4 μL particle solution was dropped on a carbon-coated copper grid and incubated for 20 minutes. Excess solution was removed with a small filter paper and the sample air-dried before observation with a TEM.

Fabrication of LbL film

A smooth titanium substrate was acquired by vapor deposition of titanium onto silica surface. The substrate was ultrasound-cleaned sequentially with acetone, ethanol, and deionized water and blow-dried with nitrogen. The LbL film was fabricated according to a previous report.[25] Briefly, the PEI aqueous solution (10 mg/mL, pH 7) was first absorbed onto the substrate for 20 minutes and washed with ultrapure water twice. After the precursor layer was established, the substrate was sequentially treated with HA (1 mg/mL in 0.2 M sodium acetate buffer), washed with sodium acetate buffer, covered by CS/siRNA nanoparticles, and washed with buffer to remove excess polymers. HA and CS/siRNA were each defined as one monolayer and HA-CS/siRNA was defined as one bilayer. Except during the first bilayer, in which the CS/siRNA was incubated for different times, each monolayer was incubated for 10 minutes. The steps were repeated until a desired number of bilayers was obtained.

Dynamic contact angle measurement

During growth of the film, the water contact angle of each monolayer was analyzed with a DSA100 drop shape analysis system, KRÜSS GmbH (Hamburg, Germany). Before measurement, the sample was dried with nitrogen and analyzed immediately. The drop shape was snapped with a camera and the contact angle was calculated with the software provided by the manufacturer.

Atom force microscope observation

The surface topography of each bilayer was observed with a commercial Digital Instruments Nanoscope IIIa Multi-Mode SPM (Veeco Instruments, Santa Barbara, CA, USA) under ambient conditions after drying with nitrogen. Five random spots of each bilayer were scanned and the images were analyzed by using commercial Scanning Probe Image Processor (SPIP) version 6.0 software Image Metrology A/S (Hørsholm, Denmark). The average roughness (S_a) was used to indicate the roughness of the surface. The calculation of the all S_a occurred after the image correction by a second-order polynomial plane fit, where M=N=512.

$$S_a = \frac{1}{MN}\sum_{k-0}^{M-1}\sum_{i-0}^{N-1}[z(x_k, y_i)]$$

Note also that roughness values depend strongly on measurement conditions, especially scan range. Here, the scan ranges were 2×2 μm for all samples.

Scanning electron microscope observation

The growth of the LbL film was observed continuously using a scanning electron microscope ([SEM] S4800). Briefly, each formulated bilayer was dried with nitrogen immediately and sputter-coated with platinum in a vacuum chamber. The specimen was then observed with an SEM at randomly selected scopes and representative images were taken.

Quantification of siRNA in the film

To measure the siRNA amount incorporated in the LbL films, 10 μL CS/siRNA nanoparticles were dropped cautiously on the HA surface and incubated for a designated period of time. The remaining solution was carefully collected into a microtube by pipette. Afterwards, the adsorbed nanoparticles were washed twice by sodium acetate buffer with 10 μL each time and the spent buffer was also collected into the above microtube to perform the quantification analysis. The quantification of siRNA was performed by RiboGreen assay according to the manufacturer's instructions. Briefly, the collected sample was diluted to 100 μL with TE buffer and mixed with 100 μL diluted RiboGreen (1:200 with TE buffer) in black-bottom 96-well plates in a dark condition. Then the plate was read with a fluorescent plate reader at 485/530 nm (excitation/emission) wavelengths. The siRNA incorporated in the film was calculated by subtracting the collected sample from the original 10 μL CS/siRNA nanoparticles. The total amount of siRNA in the film was calculated manually by adding up the amount in each bilayer.

Release profile

To analyze the release profile of the film, titanium coated with LbL film was immersed in 200 μL phosphate-buffered saline (PBS) in a 48-well plate and incubated at 37°C in 5% CO_2 and 100% humidity. At designated time points, the PBS was collected and immediately replaced with fresh buffer. The released siRNA in the suspension was quantified with RiboGreen assay as described above.

Sustained gene silencing from the LbL film

The silencing efficiency was determined in GFP-positive H1299 (half-life 2 hours, kindly provided by Dr Anne Chauchereau [CNRS, Villejuif, France]), which was maintained in Dulbecco's Modified Eagle's Medium, 10% fetal bovine serum, 1% penicillin/streptomycin, and 0.2% Geneticin®. To evaluate the GFP silencing effect from the film, CS/siGFP was used to construct the LbL film. Meanwhile, the siTNF was used as siRNA negative control (siNC). Both CS/siNC nanoparticles and blank CS were built up with the same method. Also, Lipofectamine 2000 and CS delivery systems were included and naked titanium was set as blank control. The cells were seeded on titanium coated with the film in 48-well plates at a density of 10,000 cells per well and cultured for 3, 5, and 7 days. At the desired point, the medium was removed and cells were fixed with 4% paraformaldehyde. The green fluorescence intensity was observed by confocal laser scanning microscope (LSM 700; Carl Zeiss Meditec AG, Jena, Germany) to evaluate the knockdown efficiency of GFP.

To quantify the knockdown efficiency, cells at desired time points were harvested by the typical trypsin method, and the green fluorescence intensity was measured by a Gallios™ Flow Cytometer (Beckman Coulter, Indianapolis, IN, USA). Fluorescence intensity was referenced to cell count and gating was applied to select viable cells. The geometric mean was taken as the value of fluorescence intensity and the data were presented as percentage of the blank control.

Cell viability assay

To evaluate the viability, alamarBlue® assay was performed according to the manufacturer's instructions. Briefly, the reaction medium was prepared with the mixture of medium and alamarBlue at 10:1 ratio prior to use. At designated time points, the medium was removed and cells were treated with 200 μL reaction medium in each well. After incubation for 2 hours in the cell culture incubator, the medium was transferred to a 96-well plate and the fluorescence intensity was measured by plate reader at 560/590 nm (excitation/emission) wavelengths. The data were presented as the ratio to the blank control.

Cellular internalization

The uptake of CS/siRNA nanoparticles was determined both in H1299 and MG63 cells cultured on the naked titanium surface in 48-well plates at a density of 10,000 cells/well. Cyanine 5 (Cy5)-labeled siRNA was used to form the nanoparticles to transfect the cells at a final siRNA concentration of 80 nM. After 24 hours' transfection, the medium was removed and the cells were washed with PBS and fixed with 4% paraformaldehyde for 20 minutes. The fixed cells were then stained with Hoechst according to the manufacturer's protocol and washed with PBS thrice to remove excess dye. The sample was turned over and placed on a cover glass to be observed by confocal laser scanning microscopy.

Osteogenic differentiation

The osteogenic potency of LbL film in MG63 cells was checked by siCkip-1 incorporation. Briefly, cells were seeded at a concentration of 10,000 cells/well in a 48-well plate and allowed 3 days' proliferation. The osteogenic medium containing 10 mM β-glycerophosphate, 50 μg/mL ascorbic acid, and 10^{-7} M dexamethasone was then used to perform osteogenic induction. After 2 weeks' induction, samples were fixed in 4% paraformaldehyde for 20 minutes and stained by BCIP/NBT, Sirius Red, and Alizarin Red, respectively. After rinsing with abundant distilled water, the samples were observed by stereomicroscope (Leica Microsystems, Wetzlar, Germany). The related gray scales of images were further analyzed by Image J software.

Statistical analysis

Three independent biological samples were repeated in each test and the results were presented as mean ± standard deviation. One way analysis of variance and Student–Newman–Keuls q-test was used to compare the average, and $P<0.05$ was considered significant.

Results

Size and morphology of CS/siRNA nanoparticles

As shown in Figure 1A, the CS/siRNA nanoparticles had a symmetric size distribution with an average size of 147.6 nm according to dynamic light scattering-based measurements. TEM observation showed that the morphology of the nanoparticles was irregular and the size distribution extensive. Three representative nanoparticles with sizes of ~100 nm, ~200 nm, and 500 nm were chosen for analysis (Figure 1B). The shape of the particles was likely to become more spherical when the diameter increased, suggesting that the nanoparticles may be comprised of several smaller particles. This possibly results from the higher surface-to-volume ratio of a sphere, which enables maximum nanoparticle conjunction.

Contact angle measurement

The water wettability of each monolayer was monitored during the growth of the LbL film (Figure 2). The naked titanium was marked as monolayer 0, which was hydrophobic and had the highest contact angle of ~57° compared to any of the other

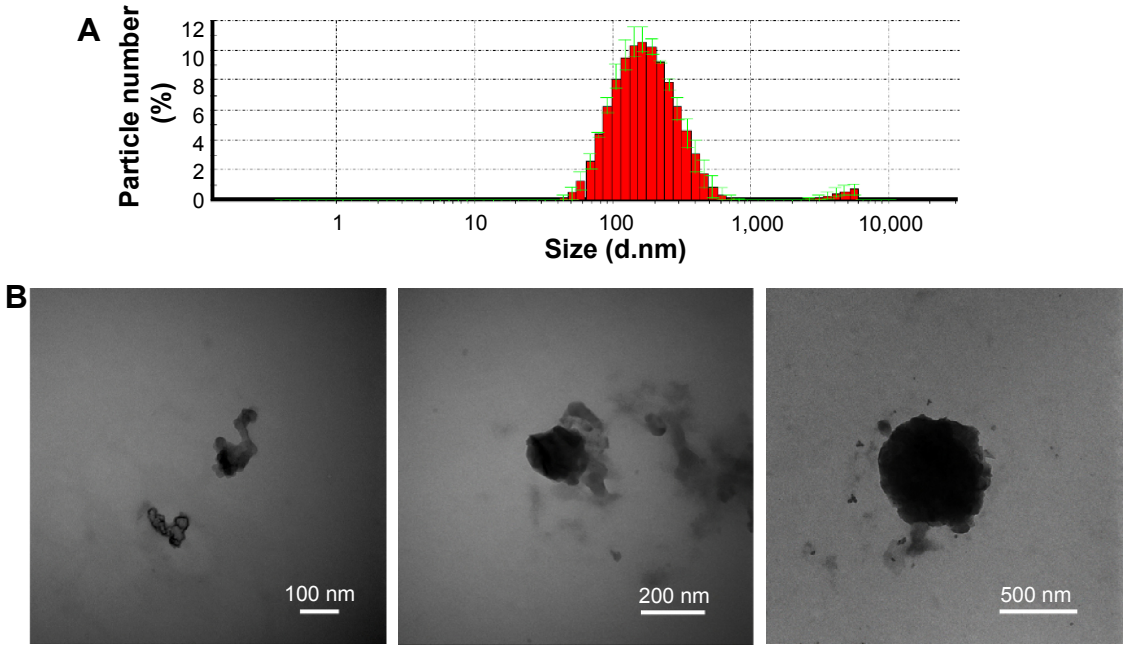

Figure 1 Chitosan/siRNA nanoparticle characterization.
Notes: (**A**) Size distribution measured by dynamic light scattering at 20°C. (**B**) Three representative transmission electron microscope images of the nanoparticles.
Abbreviation: d, diameter.

coated substrates. The initial adsorbed PEI, named monolayer 1, was hydrophilic, and the contact angle was lowered to approximately 27°. After monolayer 2 at the surface, which was sodium HA, the contact angle increased. Upon addition of alternating layers, we observed alternating increased and decreased contact angles until monolayer 17, which had CS/siRNA on the surface. HA monolayers on the surface produced lower contact angles than CS/siRNA, but none of them was higher or lower than naked titanium or PEI.

Atomic force microscopy observation

A 2×2 μm area of each bilayer was scanned by atomic force microscopy (AFM) and the images are presented as three-dimensional modes (Figure 3A). The S_a was calculated based on the

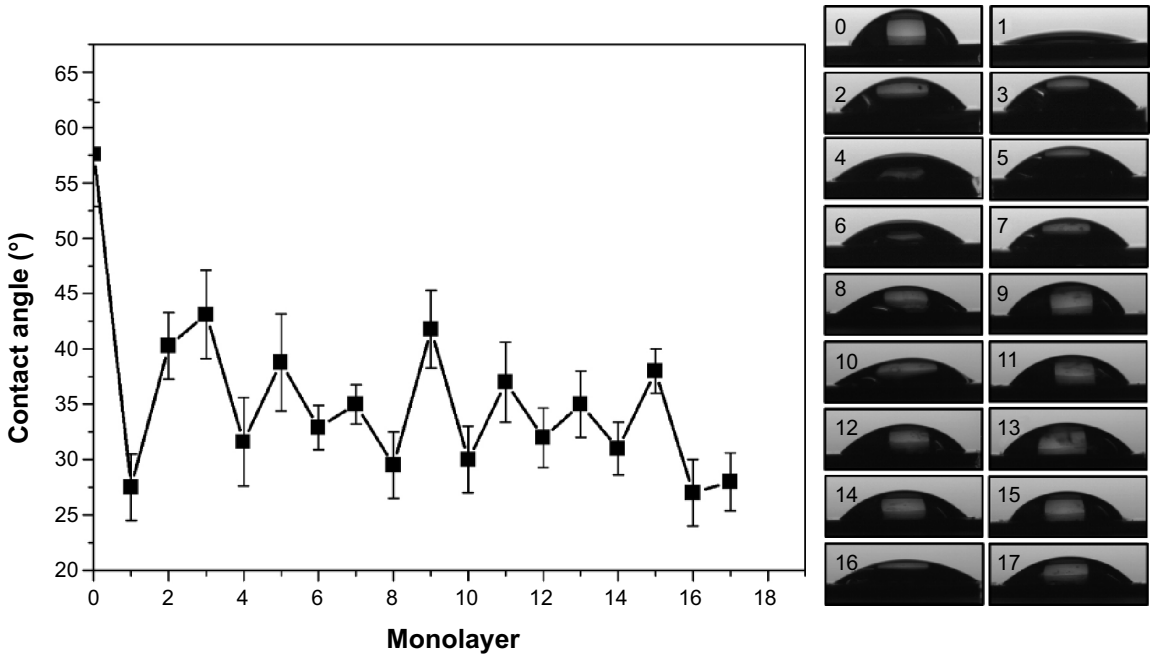

Figure 2 Water contact angle was altered during growth of the film.
Notes: The odd layer numbers represent chitosan/siRNA nanoparticles on the surface except for number 1, which is polyethylenimine. The even numbers represent sodium hyaluronate on the surface. Three independent measurements were repeated.

images (Figure 3B). The bare titanium surface (bilayer 0 in Figure 3) shows a homogeneous surface with an S_a of about ~0.6 nm. When coated with the first bilayer, the surface became even smoother with an S_a of ~0.5 nm. This might be because of the CS/siRNA nanoparticles mainly occupying the space between vapored titanium granules. The biggest height fluctuation was observed from the second bilayer where the roughness increased to ~6 nm, whereas the third and fourth bilayers showed a relatively smaller height fluctuation, with an S_a of ~3 nm and ~2.6 nm, respectively. The surface height was elevated in the fifth bilayer with an S_a of ~5 nm. Interestingly, surface roughness was returned to a low level by the addition of the last three HA-CS/siTNF bilayers, and the S_a remained at a couple of nanometers.

SEM observation

Generally, the density, thickness, and homogeneity of the film increased with the accumulation of bilayers (Figure 4). Specifically, during the first three bilayers, the CS/siRNA nanoparticles dispersedly adsorbed on substrate surface. It was notable then that the hybrid CS/siRNA nanoparticles and HA anchored together in the following three bilayers. In the final two bilayers, CS/siRNA nanoparticles closely arrayed to formulate a homogeneous thick film coating.

siRNA loading and release profile

The calibration curve and linear fitting of fluorescence versus CS/siRNA nanoparticle solution used for dilution was performed (Figure 5A). To understand if the incubation time would affect siRNA loading during the LbL procedure, the amount of siRNA loaded in the first bilayer was analyzed in detail. The load amount increased dramatically during the first 5 minutes (~0.055 μg), more slowly in the following 5 minutes (~0.015 μg), and only minor additional adsorption was observed afterwards (Figure 5B). Therefore, 10 minutes was chosen as the incubation time of each layer step to fabricate the multilayered film. The accumulated siRNA amount increased gradually with the layer number, indicating that the LbL approach could be used to control the loading amount (Figure 5C). It was exciting that the siRNA released steadily from LbL film without apparent initial burst release (Figure 5D). After 7 days' elution, ~0.3 μg in total was released, which was nearly 100%.

Sustained gene silencing and viability

Stably GFP-expressing cell line, H1299, was cultured and transfected on the titanium substrate coated with different film or treated with nanoparticles directly for different durations (Figure 6A). Three days after transfection, the GFP intensity was significantly reduced for cells grown on the siGFP-loaded film surface with effects comparable to the vectors of Lipofectamine 2000 and CS. No silencing was observed on film containing siNC, CS, or naked titanium. After 5 days of incubation, slight recovery of GFP was observed in the silenced groups. After 7 days, most GFP expression was recovered using vectors of Lipofectamine 2000 or CS. In contrast, the GFP expression remained fully suppressed for cells grown on the siGFP-loaded LbL film surface. To further quantify the gene silencing efficiency of the siRNA, flow cytometry was used to measure the green fluorescence intensity (Figure 6B). The quantitative data were in agreement to the confocal imaging result. At day 3 and day 5, LbL film, Lipofectamine 2000, and CS could silence EGFP expression by 70%–80%. This level of knockdown remained fully at day 7 for CS LbL films, whereas Lipofectamine 2000 and CS alone could not provide sustained silencing at the same level. Since cell viability might affect GFP expression, the viability was monitored in the meantime by alamarBlue® assay (Figure 6C). It was favorable that cells with all the treatments exhibited over 80% viability, implying that the LbL film was a cell compatible coating and the silencing originated from the effect of siGFP.

Cellular internalization

The cellular internalization of both MG63 and H1299 cells was observed to confirm the ability of CS to internalize siRNA into osteoblast cells. The Cy5-labeled siRNA (red) appeared as perinuclear dots (blue) when analyzed by confocal microscopy, both in H1299 and MG63 (Figure 7), indicating that the CS could also transfect osteoblasts.

Osteogenic differentiation

The osteogenic differentiation of MG63 was performed to check the osteogenic potency of LbL film containing siCkip-1 (Figure 8). The alkaline phosphatase (ALP) activity, collagen secretion, and ECM mineralization on LbL-siCkip-1 surface were all augmented enormously compared to control groups (Figure 8A). The image quantification results indicated that the robust ALP activity could be approximately fivefold, while the relative ECM mineralization was approximately fourfold compared to naked titanium (Figure 8B). The collagen secretion on LbL-siNC and LbL-CS also increased over fourfold, but it was elevated more than tenfold in the siCkip-1 group (Figure 8B).

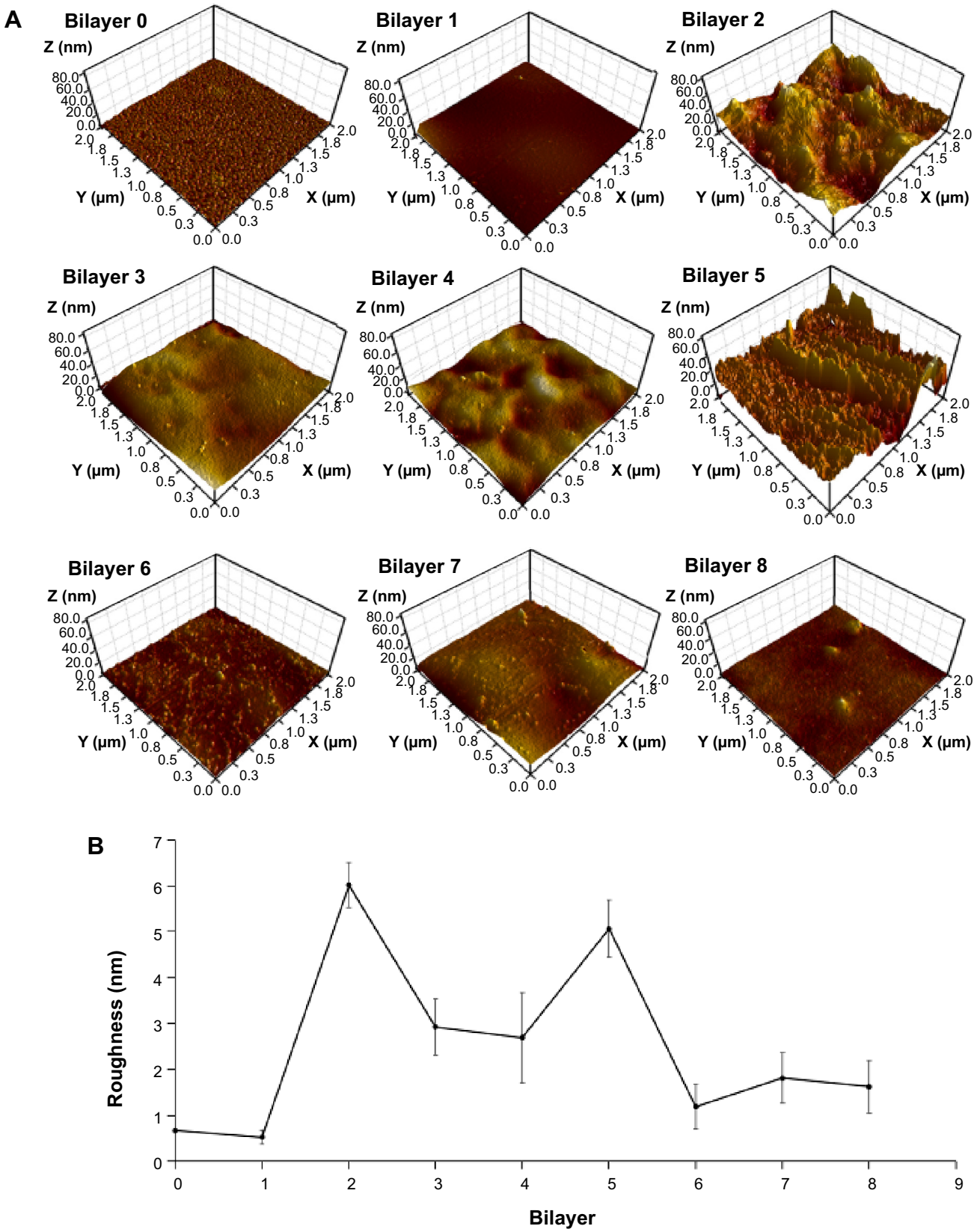

Figure 3 Surface topology of layer-by-layer film.

Notes: (**A**) The morphology of layer-by-layer films (bilayer 0 to bilayer 8) of sodium hyaluronate and chitosan/siRNA nanoparticles studied by atomic force microscopy. (**B**) The plot of calculated average roughness (S_a) versus the number of bilayers. The film was built up on the same specimen and five random spots on each bilayer were scanned.

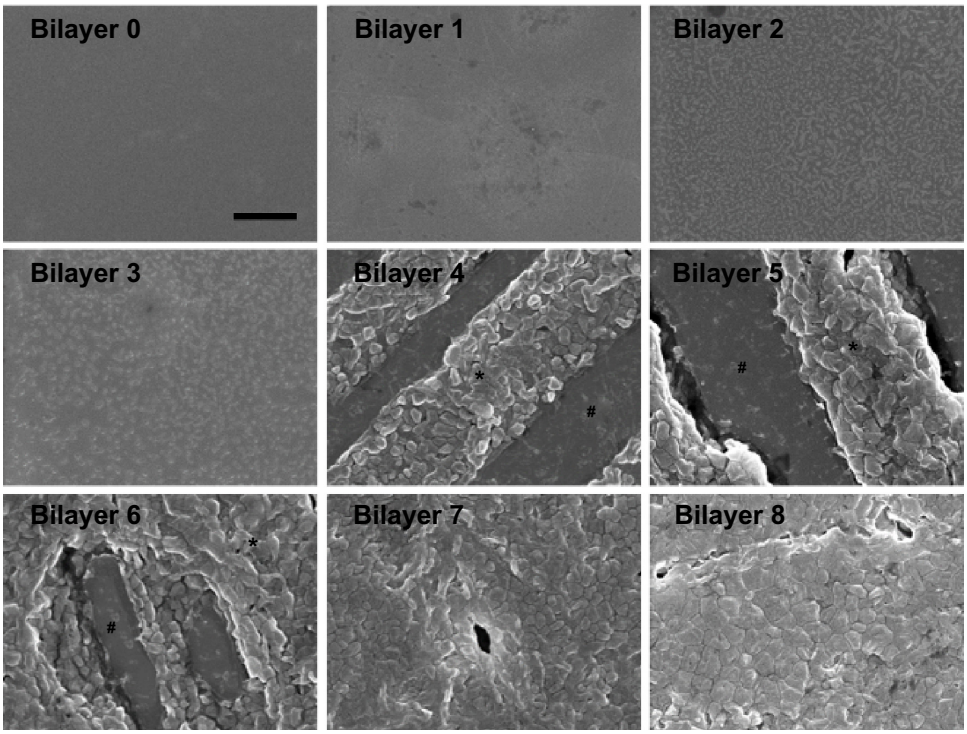

Figure 4 Scanning electron microscope observation of each bilayer.
Notes: Scale bar =1 μm. "*" and "#" represent chitosan/siRNA nanoparticles and sodium hyaluranate, respectively.

Discussion

In order to functionalize the titanium with siRNA, we adsorbed CS/siRNA nanoparticles on the ultra-smooth titanium surface using an LbL procedure. Here, we describe a feasible method to fabricate siRNA-loaded film on titanium surfaces with long-term lifetime and sustained gene silencing capacity. The CS/siRNA nanoparticles are formulated mainly by the nonspecific electrostatic force through a simple mixing procedure that results in a range of size distributions. To reveal the characteristics of the LbL film, several tests were performed. The water contact angle increased and decreased alternately upon addition of different surface layers, which has also been observed in other LbL coatings.[26,27] The alteration of the contact angle confirmed that the LbL procedure could apply different polymers sequentially to the titanium surface. According to the study by Bumgardner et al CS can, due its hydrophobic and positive charge, promote protein adsorption, thus leading to enhanced osteoblast precursor cell attachment.[28] On the contrary, hyaluronate is more hydrophilic and shows resistance to protein adsorption.[29] For this reason, we adhered CS as the final layer. AFM scanning was performed to observe the surface topography and measure the roughness, which in general exhibited an up-and-down evolution as well. It was notable that the CS/siRNA nanoparticles had a wide diameter distribution range that was over 100 nm but the AFM roughness was less than 6 nm. There are two possible reasons for this. One was the image correction by a second-order polynomial plane fit before S_a calculation, and the other one might be put down to the hybrid LbL structure, in which the gaps between nanoparticles in each layer were fulfilled by each other and resulted in small surface height. The SEM images clearly revealed that the CS/siRNA nanoparticles were anchored on top of HA polymer, which confirmed the expected LbL result. The profile of loaded siRNA was analyzed by fluorescence intensity measurement, which is the most sensitive method in RNA quantification.[30] The load amount of siRNA increased with time more rapidly at the initial stage and slowly afterwards, which can possibly be explained by the surface charge saturation. This could also explain the linear relation between the cumulative amount and the bilayer number, since the same exposure time was used. In our experiment, the release profile of the LbL film was gradual and linear within the duration of 1 week, which is consistent with the findings of another report.[31] The electrostatically anchored multilayer structure provided a controlled release of the loading cargo, which is pivotal for local drug delivery in order to obtain a sustained effect.[32–34]

H1299 originates from epithelial lung cancer and has a prominent ability of endocytosis. Therefore, it is an ideal cell line for validating CS parameters for siRNA delivery.[35]

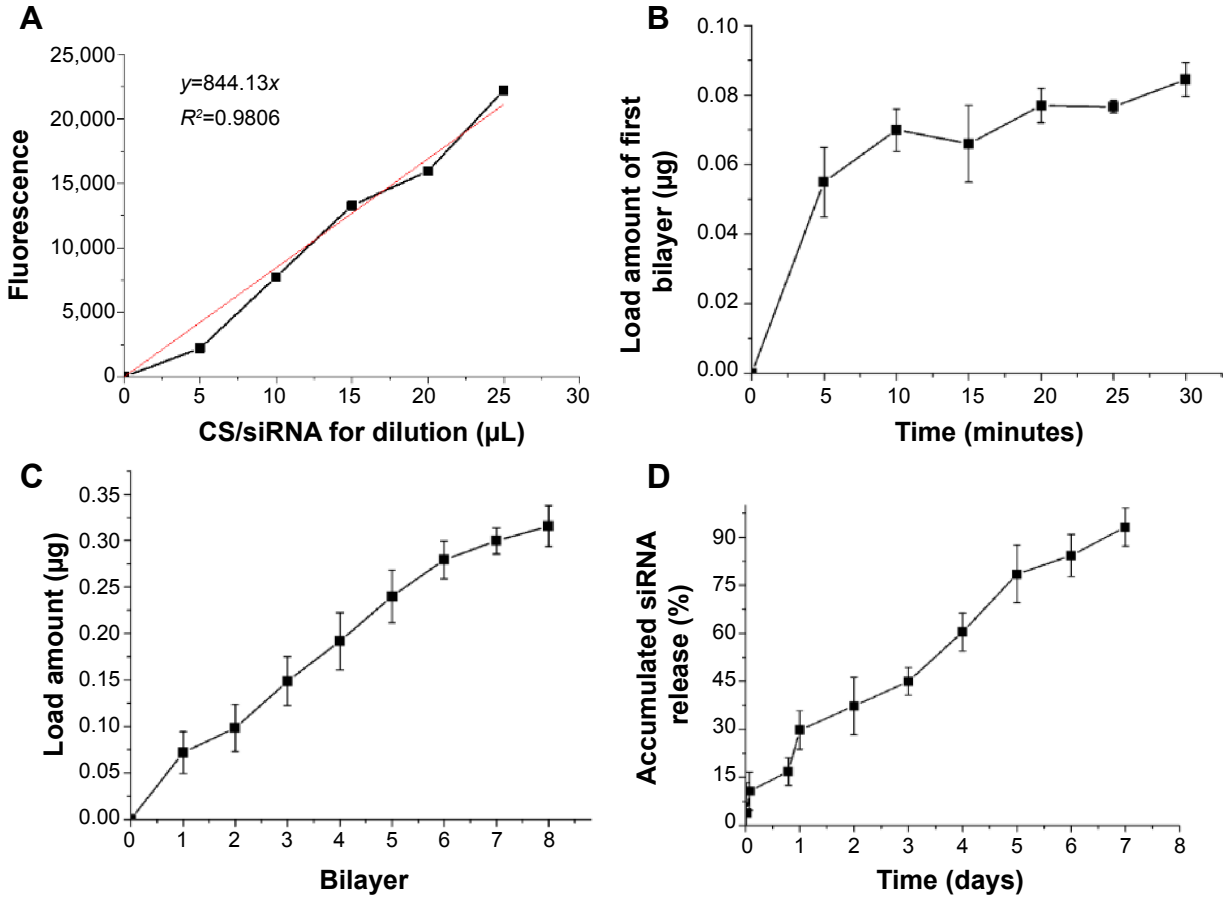

Figure 5 Quantification of siRNA on the titanium surface.
Notes: (**A**) Calibration curve and linear fitting of fluorescence versus the amount of chitosan (CS)/siRNA nanoparticle solution used for dilution. (**B**) The amount of siRNA in the first bilayer with different incubation times. (**C**) Accumulated siRNA loading amount with increased number of bilayers. (**D**) Accumulated siRNA release profile.

We have observed that the LbL-siGFP, Lipofectamine 2000/siGFP, and CS/siGFP were significantly lower in relative GFP fluorescence intensity than the LbL-siNC, LbL-CS, and naked titamium. This indicates that the siGFP activity remains intact after LbL deposition and the silencing effect is comparable to conventional nanoparticle-mediated transfection. Despite the sustained lower GFP expression obtained in our study, the possible viability influence must be excluded since lower viability can also result in lower GFP expression. Excitingly, the LbL film has no significant cytotoxicity upon the H1299 and the suppression of GFP mainly originates from the siGFP effect. To uncover the potential osteogenic promotion ability of the LbL film, the well-documented siCkip-1 served as function molecule.[23] Ckip-1 is a newly discovered intracellular negative regulator of bone formation that does not affect bone resorption, and downregulation of Ckip-1 by siCkip-1 can significantly promote osteogenesis both in normal and osteoporotic conditions.[36] The osteogenic differentiation markers of ALP production, collagen secretion, and ECM mineralization, which are determined by the intensity of staining color, were all enhanced. It is notable that the LbL-siNC and LbL-CS appeared to have a higher collagen secretion ability than the naked titanium. This can possibly be explained by the fact that, during the LbL accumulation, CS molecules increased to a certain amount that could promote osteoblast behavior.[37] In the meanwhile, since siCkip-1 is a proven effective drug for osteoporosis treatment, the modified titanium might be used to promote osseointegration under the osteoporotic condition as well.

Conclusion

LbL self-assembly is a convenient technique by which to fabricate multilayered thin film on biomaterial surface. In our study, CS/siRNA nanoparticles were used with an LbL technique to engineer the surface of titanium, which is the main applied biomaterial in implantology due to its excellent bone binding ability. The quantification of loaded siRNA showed a linear relationship with bilayer number and the formulated film could degrade gradually and release the siRNA in a sustained fashion over 1 week

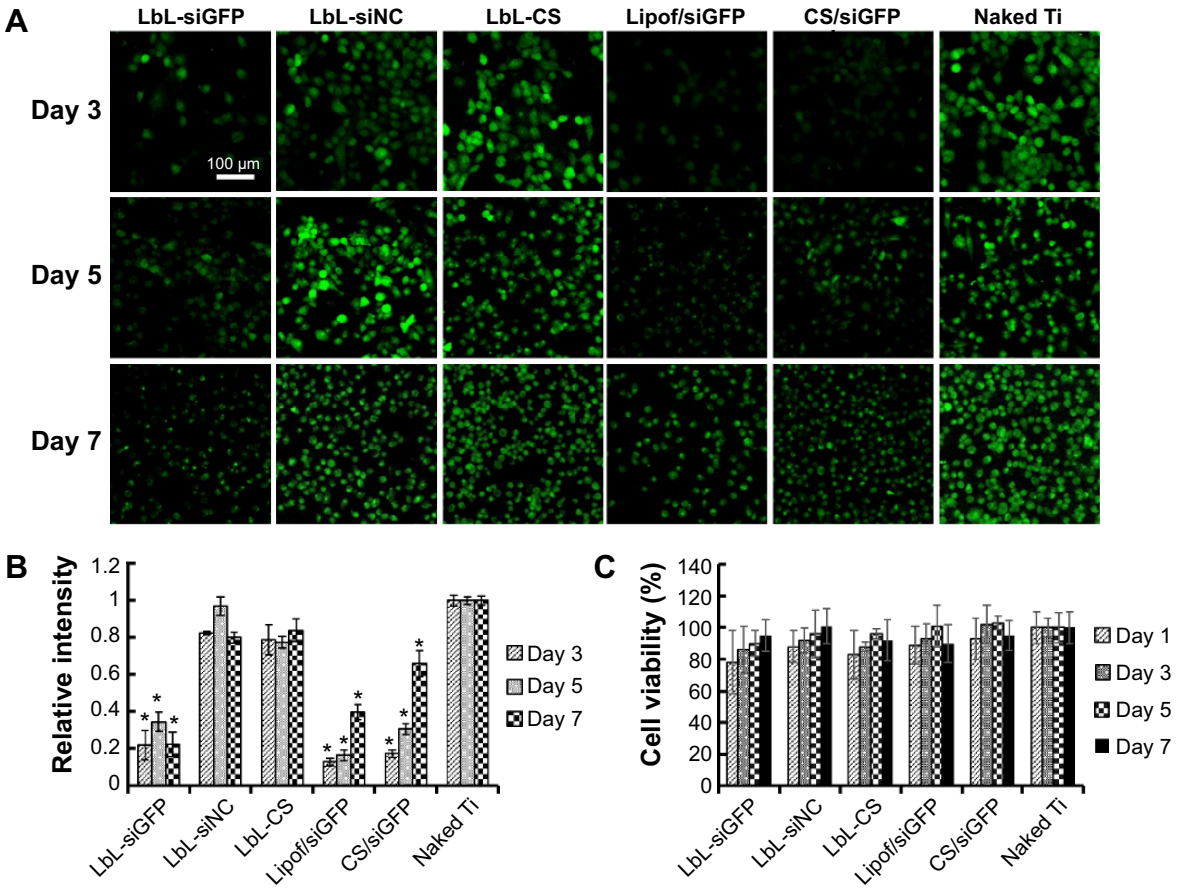

Figure 6 Knockdown and cytotoxicity in H1299 cells.
Notes: (**A**) The knockdown efficiency of GFP visualized with a confocal laser scanning microscope (scale bar =100 μm). (**B**) Knockdown efficiency quantified by flow cytometry. *$P<0.05$ compared to naked Ti. (**C**) Cellular viability carried out by alamarBlue® assay.
Abbreviations: CS, chitosan; LbL, layer-by-layer; Lipof, Lipofectamine® 2000; siGFP, siRNA targeting the expression of GFP; siNC, siRNA negative control.

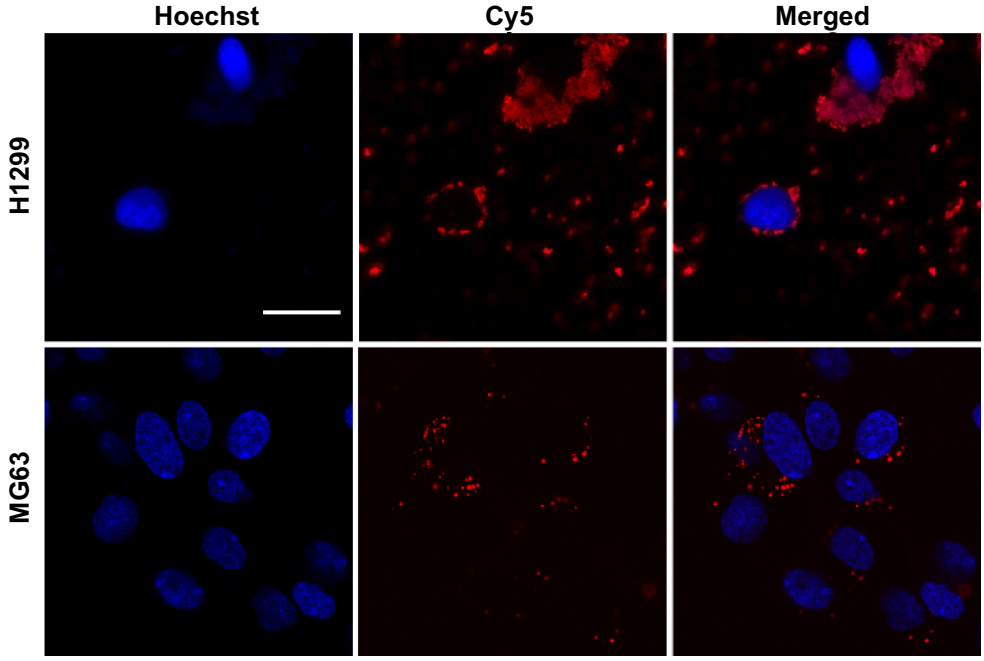

Figure 7 Cellular internalization in H1299 and MG63 cells.
Note: Scale bar =25 μm.

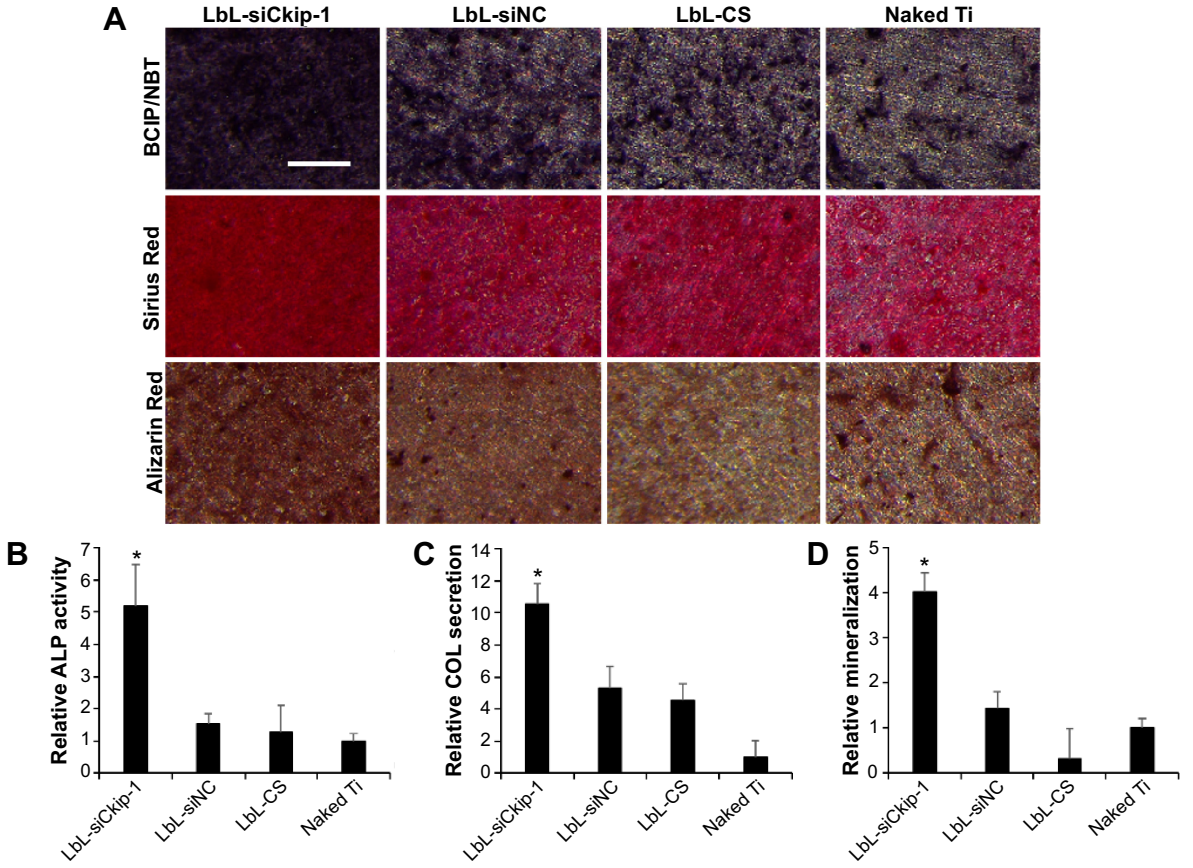

Figure 8 Osteogenic differentiation of MG63 cells.
Notes: (**A**) ALP, COL, and mineralization by BCIP/NBT, Sirius Red and Alizarin Red staining respectively (scale bar =200 μm). (**B**–**D**) Quantitative information of (**A**) by Image J analysis. *$P<0.05$ compared to naked Ti.
Abbreviations: ALP, alkaline phosphatase; COL, collagen; CS, chitosan; LbL, layer-by-layer; siCkip-1, osteogenic siRNA targeting Ckip-1; siNC, siRNA negative control.

in PBS. The incorporated CS/siGFP nanoparticles could suppress GFP expression in H1299 constantly for nearly 1 week without significant cytotoxicity. The osteogenic differentiation of MG63 is considerably enhanced if siCkip-1 is embedded. Taken together, the LbL technique could be employed to introduce siRNA into titanium surface modification for better biofunction.

Acknowledgments

The work is supported by grants from the National Natural Science Foundation of China (NSFC numbers 31170915 and 81470785) and The Lundbeck Foundation Nanomedicine Centre for Individualized Management of Tissue Damage and Regeneration (LUNA). We thank Qiang Li for the sample preparation and Dan Xia for her help in contact angle measurement. We thank Menglin Chen, Claus Bus, and Lingzhou Zhao for their excellent technical assistance. The authors appreciate the Department of Oral and Maxillofacial Surgery, School of Stomatology, The Fourth Military Medical University.

Disclosure

The authors report no conflicts of interest in this work.

References

1. Wang CK, Lin JH, Ju CP, Ong HC, Chang RP. Structural characterization of pulsed laser-deposited hydroxyapatite film on titanium substrate. *Biomaterials.* 1997;18(20):1331–1338.
2. Choi JM, Kim HE, Lee IS. Ion-beam-assisted deposition (IBAD) of hydroxyapatite coating layer on Ti-based metal substrate. *Biomaterials.* 2000;21(5):469–473.
3. Szmukler-Moncler S, Perrin D, Ahossi V, Magnin G, Bernard JP. Biological properties of acid etched titanium implants: effect of sandblasting on bone anchorage. *J Biomed Mater Res B Appl Biomater.* 2004;68(2):149–159.
4. Li LH, Kong YM, Kim HW, et al. Improved biological performance of Ti implants due to surface modification by micro-arc oxidation. *Biomaterials.* 2004;25(14):2867–2875.
5. Zhao L, Liu L, Wu Z, Zhang Y, Chu PK. Effects of micropitted/nanotubular titania topographies on bone mesenchymal stem cell osteogenic differentiation. *Biomaterials.* 2012;33(9):2629–2641.
6. Zhao L, Mei S, Chu PK, Zhang Y, Wu Z. The influence of hierarchical hybrid micro/nano-textured titanium surface with titania nanotubes on osteoblast functions. *Biomaterials.* 2010;31(19):5072–5082.
7. Fenoglio I, Fubini B, Ghibaudi EM, Turci F. Multiple aspects of the interaction of biomacromolecules with inorganic surfaces. *Adv Drug Deliv Rev.* 2011;63(13):1186–1209.

8. Kim TI, Jang JH, Kim HW, Knowles JC, Ku Y. Biomimetic approach to dental implants. *Curr Pharm Des.* 2008;14(22):2201–2211.
9. Yoshinari M, Oda Y, Ueki H, Yokose S. Immobilization of bisphosphonates on surface modified titanium. *Biomaterials.* 2001;22(7):709–715.
10. Swanson TE, Cheng X, Friedrich C. Development of chitosan-vancomycin antimicrobial coatings on titanium implants. *J Biomed Mater Res A.* 2011;97(2):167–176.
11. Haimovich G, Choder M, Singer RH, Trcek T. The fate of the messenger is pre-determined: a new model for regulation of gene expression. *Biochim Biophys Acta.* 2013;1829(6–7):643–653.
12. Dorsett Y, Tuschl T. siRNAs: applications in functional genomics and potential as therapeutics. *Nat Rev Drug Discov.* 2004;3(4):318–329.
13. Elbashir SM, Harborth J, Lendeckel W, Yalcin A, Weber K, Tuschl T. Duplexes of 21-nucleotide RNAs mediate RNA interference in cultured mammalian cells. *Nature.* 2001;411(6836):494–498.
14. Joddar B, Albayrak A, Kang J, Nishihara M, Abe H, Ito Y. Sustained delivery of siRNA from dopamine-coated stainless steel surfaces. *Acta Biomater.* 2013;9(5):6753–6761.
15. Ma L, Zhou J, Gao C, Shen J. Incorporation of basic fibroblast growth factor by a layer-by-layer assembly technique to produce bioactive substrates. *J Biomed Mater Res B Appl Biomater.* 2007;83(1):285–292.
16. Lin QK, Ren KF, Ji J. Hyaluronic acid and chitosan-DNA complex multilayered thin film as surface-mediated nonviral gene delivery system. *Colloids Surf B Biointerfaces.* 2009;74(1):298–303.
17. Jewell CM, Lynn DM. Multilayered polyelectrolyte assemblies as platforms for the delivery of DNA and other nucleic acid-based therapeutics. *Adv Drug Deliv Rev.* 2008;60(9):979–999.
18. Recksiedler CL, Deore BA, Freund MS. A novel layer-by-layer approach for the fabrication of conducting polymer/RNA multilayer films for controlled release. *Langmuir.* 2006;22(6):2811–2815.
19. Ariga K, Lvov YM, Kawakami K, Ji Q, Hill JP. Layer-by-layer self-assembled shells for drug delivery. *Adv Drug Deliv Rev.* 2011;63(9):762–771.
20. Tan YF, Mundargi RC, Chen MHA, et al. Layer-by-Layer Nanoparticles as an Efficient siRNA Delivery Vehicle for SPARC Silencing. *Small.* 2014;10(9):1790–1798.
21. Elbakry A, Zaky A, Liebl R, Rachel R, Goepferich A, Breunig M. Layer-by-layer assembled gold nanoparticles for siRNA delivery. *Nano Lett.* 2009;9(5):2059–2064.
22. Hartmann H, Hossfeld S, Schlosshauer B, et al. Hyaluronic acid/chitosan multilayer coatings on neuronal implants for localized delivery of siRNA nanoplexes. *J Control Release.* 2013;168(3):289–297.
23. Zhang G, Guo B, Wu H, et al. A delivery system targeting bone formation surfaces to facilitate RNAi-based anabolic therapy. *Nat Med.* 2012;18(2):307–314.
24. Howard KA, Paludan SR, Behlke MA, Besenbacher F, Deleuran B, Kjems J. Chitosan/siRNA nanoparticle-mediated TNF-alpha knockdown in peritoneal macrophages for anti-inflammatory treatment in a murine arthritis model. *Mol Ther.* 2009;17(1):162–168.
25. Hossfeld S, Nolte A, Hartmann H, et al. Bioactive coronary stent coating based on layer-by-layer technology for siRNA release. *Acta Biomater.* 2013;9(5):6741–6752.
26. Hu Y, Cai K, Luo Z, et al. Surface mediated in situ differentiation of mesenchymal stem cells on gene-functionalized titanium films fabricated by layer-by-layer technique. *Biomaterials.* 2009;30(21):3626–3635.
27. Costa RR, Custódio CA, Arias FJ, Rodríguez-Cabello JC, Mano JF. Layer-by-layer assembly of chitosan and recombinant biopolymers into biomimetic coatings with multiple stimuli-responsive properties. *Small.* 2011;7(18):2640–2649.
28. Bumgardner JD, Wiser R, Elder SH, Jouett R, Yang Y, Ong JL. Contact angle, protein adsorption and osteoblast precursor cell attachment to chitosan coatings bonded to titanium. *J Biomater Sci Polym Ed.* 2003;14(12):1401–1409.
29. Ombelli M, Costello L, Postle C, et al. Competitive protein adsorption on polysaccharide and hyaluronate modified surfaces. *Biofouling.* 2011;27(5):505–518.
30. Jones LJ, Yue ST, Cheung CY, Singer VL. RNA quantitation by fluorescence-based solution assay: RiboGreen reagent characterization. *Anal Biochem.* 1998;265(2):368–374.
31. Castleberry S, Wang M, Hammond PT. Nanolayered siRNA dressing for sustained localized knockdown. *ACS Nano.* 2013;7(6):5251–5261.
32. Luo J, Cao S, Chen X, et al. Super long-term glycemic control in diabetic rats by glucose-sensitive LbL films constructed of supramolecular insulin assembly. *Biomaterials.* 2012;33(33):8733–8742.
33. Wohl BM, Engbersen JF. Responsive layer-by-layer materials for drug delivery. *J Control Release.* 2012;158(1):2–14.
34. Shukla A, Fang JC, Puranam S, Hammond PT. Release of vancomycin from multilayer coated absorbent gelatin sponges. *J Control Release.* 2012;157(1):64–71.
35. Liu X, Howard KA, Dong M, et al. The influence of polymeric properties on chitosan/siRNA nanoparticle formulation and gene silencing. *Biomaterials.* 2007;28(6):1280–1288.
36. Guo B, Zhang B, Zheng L, et al. Therapeutic RNA interference targeting CKIP-1 with a cross-species sequence to stimulate bone formation. *Bone.* 2014;59:76–88.
37. Ho MH, Liao MH, Lin YL, Lai CH, Lin PI, Chen RM. Improving effects of chitosan nanofiber scaffolds on osteoblast proliferation and maturation. *Int J Nanomedicine.* 2014;9:4293–4304.